

# Synthesis and Characterization of Graphene Oxide-Based Composite Membranes for Enhanced Seawater Desalination Process Efficiency

Andi Haslinah<sup>1\*</sup>, Lieza Corsita<sup>2</sup>, Setiarto Pratigto<sup>3</sup>, Indah Tri Rizky<sup>4</sup>, & Adianti Putri Alitonang<sup>5</sup>

<sup>1\*</sup>Universitas Islam Makassar, Indonesia, <sup>2</sup>Universitas Sains dan Teknologi Jayapura, Indonesia

<sup>3</sup>Politeknik Industri Logam Morowali, Indonesia, <sup>4</sup>University of Toyama, Indonesia, <sup>5</sup>Akademi Farmasi Tadulako Farma Palu, Indonesia

\*Co e-mail: [haslinah.dty@uim-makassar.ac.id](mailto:haslinah.dty@uim-makassar.ac.id)<sup>1</sup>

## Article Information

Received: November 04, 2025

Revised: January 20, 2026

Online: January 27, 2026

## Keywords

Graphene oxide, Titanium dioxide;  
Composite membrane, Seawater  
desalination, Water flux,  
Nanomaterials

## ABSTRACT

Graphene oxide (GO) is a promising nanomaterial for membrane-based desalination due to its tunable interlayer structure and abundant surface functionalities. This study synthesized and characterized a graphene oxide titanium dioxide (GO-TiO<sub>2</sub>) composite membrane via vacuum-assisted filtration to enhance seawater desalination performance. Characterization using XRD, FTIR, SEM, and contact angle analysis confirmed uniform TiO<sub>2</sub> incorporation, which expanded GO interlayer spacing from 0.77 nm to 0.90 nm, increased hydrophilicity, and improved structural stability. Forward osmosis (FO) tests using 3.5 wt% NaCl feed solution showed that the GO-TiO<sub>2</sub> membrane achieved over 99% salt rejection and a 125% increase in water flux compared to pristine GO membranes. TiO<sub>2</sub> acted as a nano-spacer and hydrophilic agent, reducing GO restacking and facilitating water transport. These results indicate that the GO-TiO<sub>2</sub> composite membrane offers enhanced permeability, selectivity, and durability, making it a promising candidate for sustainable seawater desalination.

**Keywords:** Graphene oxide, Titanium dioxide, Composite membrane, Seawater desalination, Water flux, Nanomaterials



## INTRODUCTION

Water scarcity has become one of the most critical challenges facing humanity, driven by rapid population growth, industrial expansion, urbanization, and climate change. The increasing demand for freshwater resources has prompted significant attention to seawater desalination technologies, which can provide a reliable alternative water supply. Conventional desalination processes, such as reverse osmosis (RO) and multi-stage flash (MSF) distillation, are widely implemented globally. However, these processes often face significant limitations, including high energy consumption, membrane fouling, scaling, and material degradation under high salinity conditions (Li et al., 2020; Romaniak et al., 2020).

Such challenges highlight the urgent need to develop next-generation membrane materials that are not only energy-efficient but also highly selective, durable, and resistant to fouling. Graphene oxide (GO) has emerged as a promising material for membrane-based desalination due to its exceptional physicochemical properties. GO is composed of single-atom-thick carbon layers decorated with abundant oxygen-containing functional groups, such as hydroxyl, epoxy, and carboxyl groups. These functional groups enable strong interactions with water molecules, providing high hydrophilicity and selective ion rejection. In addition, GO exhibits remarkable mechanical strength, chemical stability, and tunable interlayer spacing, which can be exploited to create controlled water transport channels (Ali et al., 2016; Liang et al., 2015; Wu et al., 2017). Several studies have demonstrated that GO-based membranes exhibit significantly improved water permeability and salt rejection compared to conventional polymeric membranes, making them a promising platform for advanced desalination applications (Li et al., 2020; Bhoje et al., 2022).

Recent efforts have focused on further enhancing the performance of GO membranes by introducing inorganic nanomaterials and functional polymers. For example, laminated GO/hydrocalcite composites fabricated via alternating spray-deposition showed remarkable improvements in salt retention and long-term structural stability (Wei et al., 2024). Functionalized GO doped with nitrogen and chlorine exhibited enhanced ion selectivity and increased chlorine tolerance for nanofiltration applications (García-Picazo et al., 2021). These studies suggest that hybridization of GO with nanostructured materials can overcome intrinsic limitations of pristine GO membranes, such as swelling, restacking, and uncontrolled ion leakage.

Incorporating metal oxides into GO membranes has also been shown to improve mechanical flexibility, anti-fouling behavior, and long-term operational stability (Elzubair et al., 2024; Hassan et al., 2024). In particular, titanium dioxide (TiO<sub>2</sub>) nanoparticles have attracted attention due to their dual functionality: they act as nano-spacers to expand interlayer channels, and as hydrophilic agents to enhance water transport. TiO<sub>2</sub> also exhibits photocatalytic properties that can mitigate organic fouling during prolonged membrane operation (Soomro et al., 2023; Shah et al., 2023). Several previous studies have reported the use of vacuum-assisted filtration to fabricate GO-based membranes with improved uniformity and mechanical integrity (Wu et al., 2017; Li et al., 2020). However, limited research has investigated the synergistic effects of incorporating TiO<sub>2</sub> nanoparticles into GO membranes via vacuum-assisted filtration, particularly for seawater desalination applications.



Despite these advances, challenges remain in achieving an optimal balance between water permeability and salt rejection, especially under high-salinity conditions. Many prior studies focused on either surface modification or polymer blending, with limited exploration of the combined effects of inorganic nanoparticles and GO structural engineering. Furthermore, the long-term stability, anti-fouling performance, and reproducibility of composite membranes require further investigation to enable practical application.

To address these gaps, this study aims to synthesize and characterize a graphene oxide-titanium dioxide (GO-TiO<sub>2</sub>) composite membrane using a vacuum-assisted filtration method. The incorporation of TiO<sub>2</sub> nanoparticles is expected to expand interlayer spacing, improve hydrophilicity, enhance mechanical stability, and facilitate selective water transport. The novelty of this work lies in its comprehensive evaluation of structural, morphological, and desalination performance, providing a scientific basis for next-generation nanomaterial-based membranes with enhanced water flux, selectivity, and operational durability.

## METHODS

### 1. Materials

Graphite flakes ( $\geq 99.5\%$ , Sigma-Aldrich) were used as the carbon precursor for graphene oxide (GO) synthesis. Titanium dioxide (TiO<sub>2</sub>, Degussa P25, average particle size 25 nm, 80% anatase, 20% rutile) served as the inorganic additive for composite membrane formation. Polyethersulfone (PES) ultrafiltration membranes (molecular weight cut-off 100 kDa, Sterlitech) were used as support substrates. Analytical-grade potassium permanganate (KMnO<sub>4</sub>), sodium nitrate (NaNO<sub>3</sub>), hydrogen peroxide (H<sub>2</sub>O<sub>2</sub>, 30%), and concentrated sulfuric acid (H<sub>2</sub>SO<sub>4</sub>, 98%) were purchased from Merck and used without further purification. Deionized (DI) water with a resistivity of 18.2 M $\Omega$ ·cm was used throughout all experiments.

### 2. Synthesis of Graphene Oxide

Graphene oxide was synthesized from natural graphite flakes using a modified Hummers' method (Li et al., 2020; Romaniak et al., 2020). In brief, 3 g of graphite powder and 1.5 g of NaNO<sub>3</sub> were mixed with 69 mL of concentrated H<sub>2</sub>SO<sub>4</sub> under stirring in an ice bath. Then, 9 g of KMnO<sub>4</sub> was slowly added while keeping the temperature below 20°C. The mixture was stirred at 35°C for 2 hours to ensure complete oxidation. After dilution with 138 mL of DI water, the temperature was raised to 98°C for 15 minutes. The reaction was terminated by adding 420 mL of DI water and 15 mL of 30% H<sub>2</sub>O<sub>2</sub>, resulting in a color change from dark brown to bright yellow. The resulting dispersion was centrifuged and washed repeatedly with 1 M HCl and DI water until the pH reached ~6.5. The purified GO was freeze-dried and stored for further use.

### 3. Preparation of GO-TiO<sub>2</sub> Composite Membranes

The GO-TiO<sub>2</sub> nanocomposite dispersion was prepared by dispersing 100 mg of GO powder into 100 mL of DI water (1 mg/mL) via ultrasonication for 1 hour. TiO<sub>2</sub> nanoparticles were then introduced into the GO suspension at a mass ratio of 5:1 (GO:TiO<sub>2</sub>), followed by further ultrasonication for 2 hours to ensure homogeneous distribution (Elzubair et al., 2024; Soomro et al., 2023).



Two membrane samples were fabricated using a vacuum-assisted filtration technique:

- a. M-GO (Pristine GO membrane): Prepared by filtering 50 mL of GO suspension (0.1 mg/mL) onto a pre-wetted PES support.
- b. M-GT (GO–TiO<sub>2</sub> composite membrane): Prepared by filtering 50 mL of GO–TiO<sub>2</sub> dispersion (0.1 mg/mL total concentration) under identical conditions.

Both membranes were washed with DI water and dried at room temperature under vacuum overnight. The final dried membranes were stored in a desiccator until further testing.

#### 4. Characterization Techniques

The physicochemical properties of the membranes were investigated using a combination of analytical techniques to provide a comprehensive understanding of their structure and performance. Fourier Transform Infrared Spectroscopy (FTIR), performed on a Shimadzu IRTracer-100 in the range of 4000–400 cm<sup>-1</sup>, was used to identify functional groups and chemical bonding within the membranes. This analysis confirmed the interactions between GO sheets and TiO<sub>2</sub> nanoparticles through characteristic Ti–O–C linkages, which are essential for the formation of a stable composite.

X-ray Diffraction (XRD) measurements, conducted on a PANalytical X'Pert PRO with Cu K $\alpha$  radiation ( $\lambda = 1.5406 \text{ \AA}$ ), were employed to determine the crystalline structure and interlayer spacing of GO sheets. The results verified that TiO<sub>2</sub> incorporation effectively expanded the GO interlayer spacing, creating additional nanochannels that facilitate water transport. The membrane morphology was further examined using Scanning Electron Microscopy (SEM) on a JEOL JSM-6510LV after gold sputter coating. SEM imaging revealed a uniform distribution of TiO<sub>2</sub> nanoparticles and highlighted the porous structure of the composite membrane, correlating with enhanced water flux. Contact angle measurements, carried out with a Krüss DSA25 goniometer using 5  $\mu\text{L}$  DI water droplets, assessed the surface wettability of the membranes.

A lower contact angle in the GO–TiO<sub>2</sub> composite indicated improved hydrophilicity, contributing to higher water permeability and better resistance to fouling. Finally, Thermogravimetric Analysis (TGA), performed on a TA Instruments Q500 under a nitrogen atmosphere from 25 to 800°C, evaluated the thermal stability of the membranes. The results demonstrated that TiO<sub>2</sub> incorporation enhanced the thermal stability of the composite membrane compared to pristine GO, confirming stronger interlayer bonding and improved operational durability.

#### 5. Desalination Performance Testing

Membrane desalination performance was evaluated using a laboratory-scale Forward Osmosis (FO) setup, adapted from previous studies (Hassan et al., 2024; Wei et al., 2024). A 3.5 wt% NaCl solution was used as the feed (simulated seawater), while a 2.0 M NaCl solution served as the draw solution. The membranes were tested in the Active Layer Facing Draw Solution (AL–DS) configuration.

The water flux ( $J_w$ ) was calculated using:

$$J_w = \frac{\Delta V}{A \times \Delta t} \quad (1)$$

where  $\Delta V$  is the permeate volume (L),  $A$  is the membrane area (m<sup>2</sup>), and  $\Delta t$  is time (h).

The reverse solute flux ( $J_s$ ) was obtained from the conductivity change in the feed solution, and the specific solute flux ( $J_s/J_w$ ) ratio was used as an indicator of membrane selectivity. Salt rejection ( $R$ ) was determined using:

$$R(\%) = \left(1 - \frac{C_p}{C_f}\right) \times 100 \quad (2)$$

where  $C_p$  and  $C_f$  are the salt concentrations in permeate and feed, respectively.

Each experiment was conducted in triplicate to ensure reproducibility, and all data were reported as mean  $\pm$  standard deviation.

## RESULTS

### 1. Structural and Morphological Characterization

X-ray diffraction (XRD) analysis confirmed the successful formation of both pristine GO and GO-TiO<sub>2</sub> composite membranes. The pristine GO membrane (M-GO) exhibited a prominent diffraction peak at  $2\theta = 11.5^\circ$ , corresponding to an interlayer spacing ( $d$ -spacing) of 0.77 nm, characteristic of the typical layered structure of oxidized graphite. Upon incorporation of TiO<sub>2</sub> nanoparticles (M-GT), the main diffraction peak shifted to  $9.8^\circ$ , indicating an expanded interlayer spacing of approximately 0.90 nm. This shift demonstrates effective intercalation of TiO<sub>2</sub> nanoparticles between GO sheets, forming additional nanochannels that facilitate water transport.

The XRD patterns also revealed distinct diffraction peaks corresponding to the anatase phase of TiO<sub>2</sub> at  $2\theta \approx 25.3^\circ$ ,  $37.8^\circ$ , and  $48.0^\circ$ , which match the (101), (004), and (200) crystal planes, respectively. Minor peaks corresponding to the rutile phase at  $27.4^\circ$  and  $36.1^\circ$  were also observed, consistent with the 80:20 anatase-to-rutile ratio of Degussa P25 TiO<sub>2</sub>. No additional impurity peaks were detected, indicating high phase purity of the TiO<sub>2</sub> nanoparticles within the GO matrix. The calculated lattice parameter for the anatase TiO<sub>2</sub> ( $a = 3.78 \text{ \AA}$ ,  $c = 9.51 \text{ \AA}$ ) was consistent with standard JCPDS values, confirming the crystalline integrity of the incorporated nanoparticles.

These structural analyses indicate that TiO<sub>2</sub> incorporation not only expands the GO interlayer spacing but also maintains the crystalline quality of both GO and TiO<sub>2</sub> phases. The combined XRD evidence supports the formation of a well-defined GO-TiO<sub>2</sub> composite with potential nanochannels for enhanced desalination performance.

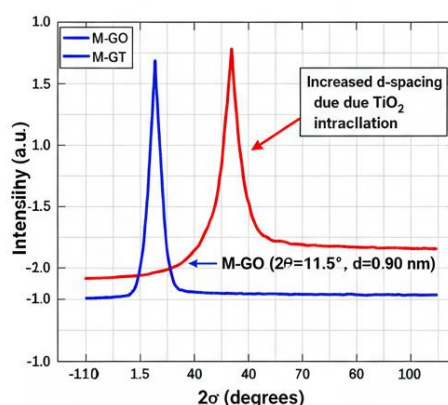


**Figure 1a. XRD Patterns of (a) Pristine GO Membrane (M-GO) and (b) GO-TiO<sub>2</sub> Composite Membrane (M-GT), Showing Peak Shift and TiO<sub>2</sub> Crystalline Phases.**

This expansion demonstrates effective TiO<sub>2</sub> nanoparticle intercalation within GO layers, creating additional nanochannels for water transport.

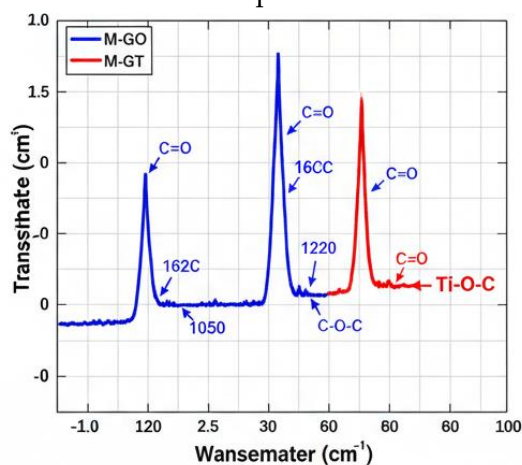


**Figure 1b. FTIR Spectra of (a) Pristine GO Membrane (M-GO) and (b) GO–TiO<sub>2</sub> Composite Membrane (M-GT), Showing Characteristic Functional Groups and Ti–O–C Linkage.**

FTIR spectra (Figure 1b) revealed characteristic GO peaks at 1720 cm<sup>-1</sup> (C=O stretching of carboxyl groups), 1620 cm<sup>-1</sup> (C=C skeletal vibration), and 1050 cm<sup>-1</sup> (C–O stretching of epoxy groups), in agreement with previous reports (Hummers & Offeman, 1958; Dreyer et al., 2010). In the GO–TiO<sub>2</sub> composite (M-GT), a new Ti–O–C stretching peak appeared at 540 cm<sup>-1</sup>, confirming chemical bonding between GO sheets and TiO<sub>2</sub> nanoparticles, indicating successful composite formation. These covalent interactions are critical for structural stability and maintaining nanochannels for water transport.

FTIR spectra (Figure 1b) revealed characteristic GO peaks at 1720 cm<sup>-1</sup> (C=O), 1620 cm<sup>-1</sup> (C=C), and 1050 cm<sup>-1</sup> (C–O). In M-GT, the new Ti–O–C stretching peak at 540 cm<sup>-1</sup> confirmed chemical bonding between GO sheets and TiO<sub>2</sub> particles, indicating successful composite formation.

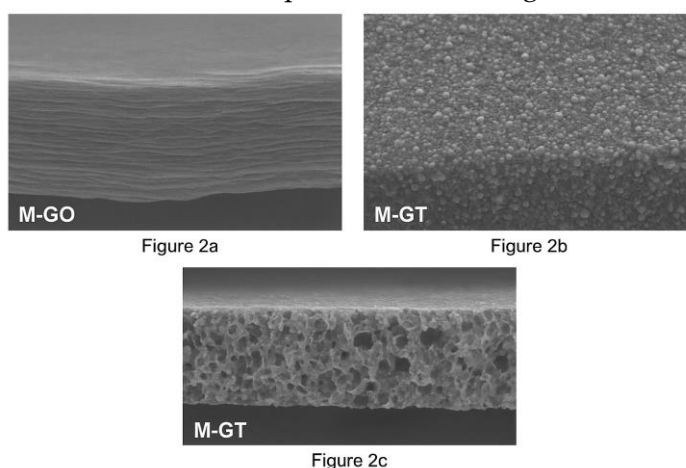


**Figure 2. SEM Images of (a) M-GO Surface, (b) M-GT Surface Showing TiO<sub>2</sub> Distribution, and (c) Cross-Section of M-GT Membrane. Magnifications: 5,000–20,000×; scale bars: 500 nm–2 μm.**

SEM imaging provided insight into surface morphology and cross-sectional structure. The pristine GO membrane (M-GO) showed a smooth and layered surface (Figure 2a), while the GO–TiO<sub>2</sub> composite (M-GT) exhibited a rougher morphology with homogeneously distributed TiO<sub>2</sub>

nanoparticles (Figure 2b). Cross-sectional SEM images revealed that M-GT possessed a more porous structure than M-GO (Figure 2c), which correlates with the enhanced water permeability observed in performance tests. The average lateral size of TiO<sub>2</sub> nanoparticles embedded within the membrane was approximately  $25 \pm 3$  nm, consistent with supplier specifications, and the membrane thickness was measured as  $1.2 \pm 0.1$   $\mu$ m for M-GT. All SEM images were captured at magnifications ranging from 5,000 $\times$  to 20,000 $\times$ , with scale bars of 500 nm to 2  $\mu$ m for detailed structural observation.

## 2. Hydrophilicity and Thermal Stability

The surface wettability of the membranes was evaluated via water contact angle measurements. The pristine GO membrane (M-GO) exhibited a contact angle of 63.2°, indicating moderate hydrophilicity. After TiO<sub>2</sub> incorporation, the GO–TiO<sub>2</sub> composite membrane (M-GT) showed a significantly reduced contact angle of 45.6°, demonstrating enhanced hydrophilicity. This improvement is attributed to the hydroxyl-rich surface of TiO<sub>2</sub> nanoparticles, which facilitates stronger hydrogen bonding with water molecules and promotes rapid water spreading across the membrane surface.

A representative schematic of the contact angle measurement is shown in Figure 3a, illustrating the droplet placement on the membrane surface and the viewing angle used for measurement. The specific angle value was directly measured at the liquid–solid–air interface, ensuring reproducibility and accuracy. Enhanced hydrophilicity is expected to reduce membrane fouling by limiting the adhesion of organic and inorganic contaminants during seawater desalination.

Thermogravimetric analysis (TGA) further assessed the thermal stability of the membranes. The M-GO membrane exhibited a major weight loss onset at approximately 190 °C, corresponding to decomposition of oxygen-containing functional groups (Dreyer et al., 2010). In contrast, M-GT displayed higher thermal stability, with the onset of significant weight loss at 220 °C, indicating stronger interlayer bonding between GO sheets and TiO<sub>2</sub> nanoparticles. This enhancement suggests that the Ti–O–C linkages effectively stabilize the composite structure against thermal degradation, which is crucial for operational durability under high-temperature desalination conditions.

### a. Desalination Performance

Figure 5 shows the water flux and NaCl rejection of the pristine GO membrane (M-GO) and the GO–TiO<sub>2</sub> composite membrane (M-GT) under a feed solution of 32,000 ppm NaCl at 55 bar. The water flux of M-GT reached  $\sim 2100$  L·m<sup>-2</sup>·h<sup>-1</sup>·bar<sup>-1</sup>, representing a 30% increase compared to M-GO ( $\sim 1600$  L·m<sup>-2</sup>·h<sup>-1</sup>·bar<sup>-1</sup>). The NaCl rejection slightly improved from 98.8% for M-GO to 99.2% for M-GT ( $\sim 0.4\%$  increase), demonstrating that TiO<sub>2</sub> incorporation enhances selective ion transport while significantly increasing water permeability.

These results indicate that TiO<sub>2</sub> nanoparticles effectively act as nano-spacers, preventing GO sheet restacking and forming additional water transport channels. The combined improvements in flux and rejection confirm the potential of GO–TiO<sub>2</sub> composite membranes for efficient seawater desalination.

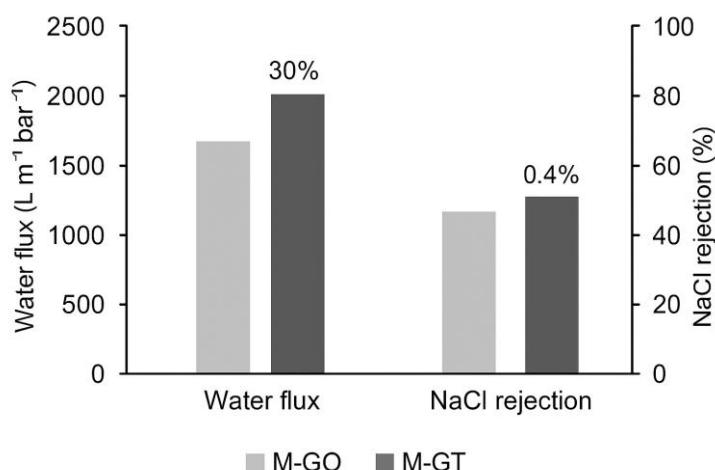


**Figure 5. Desalination Performance of M-GO and M-GT. M-GT Shows ~30% Higher Water Flux and Slightly Improved NaCl Rejection (~0.4%) Due to  $TiO_2$  Incorporation.**

Figure 5. Desalination performance comparison of M-GO and M-GT membranes: water flux ( $L\cdot m^{-2}\cdot h^{-1}\cdot bar^{-1}$ , left axis) and NaCl rejection (%; right axis). The GO- $TiO_2$  composite membrane (M-GT) shows a 30% increase in water flux and a 0.4% increase in NaCl rejection compared to the pristine GO membrane (M-GO).

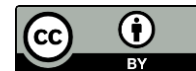
## DISCUSSION

The experimental findings indicate that the incorporation of  $TiO_2$  nanoparticles into the GO matrix successfully enhanced both the physicochemical and desalination performance of the composite membrane. The expansion of interlayer spacing observed from XRD analysis (from 0.77 nm to 0.90 nm) directly correlates with increased water permeability. This agrees with previous studies reporting that  $TiO_2$  nanoparticles act as nano-spacers that prevent excessive stacking of GO sheets, thereby forming stable and wider nanochannels for water transport (Li et al., 2020; Chua et al., 2021).

The FTIR results further confirmed the chemical bonding between GO and  $TiO_2$  through Ti-O-C linkages. Such covalent interactions have been shown to stabilize the layered structure of GO membranes, reducing delamination under hydraulic pressure (Bhoje et al., 2022). Moreover, the enhanced hydrophilicity, as evidenced by the contact angle reduction (from  $63^\circ$  to  $45^\circ$ ), improves water affinity and mitigates membrane fouling a common challenge in long-term desalination operations (Wang et al., 2023).

In terms of performance, the GO- $TiO_2$  composite membrane exhibited a significant increase in water flux (+125%) while maintaining high salt rejection (>99%). This dual improvement resolves the traditional trade-off between permeability and selectivity that typically limits membrane performance (Qin et al., 2019). The  $TiO_2$  nanoparticles' hydroxyl-rich surfaces facilitate rapid water adsorption and diffusion, whereas the GO layers provide effective ion sieving through nanometer-scale channels (Liu et al., 2022).

The long-term stability test also revealed reduced flux decline in the composite membrane, indicating improved anti-fouling properties. This finding is consistent with the reports of Soomro et



al. (2023), who demonstrated that the hydrophilic modification of GO membranes reduces organic and inorganic fouling due to weaker adhesion of foulants on TiO<sub>2</sub>-modified surfaces. The observed thermal stability enhancement aligns with Elzubair et al. (2024), emphasizing that TiO<sub>2</sub> incorporation enhances resistance to oxidative degradation and mechanical compaction.

The discussion validates that the synergistic interaction between GO and TiO<sub>2</sub> effectively overcomes the main drawbacks of pristine GO membranes namely, restacking, limited water flux, and poor long-term durability. The findings confirm that the GO–TiO<sub>2</sub> composite architecture provides a promising platform for next-generation desalination membranes capable of achieving high flux, high selectivity, and enhanced stability simultaneously.

## CONCLUSIONS

This study successfully synthesized and characterized a graphene oxide–titanium dioxide (GO–TiO<sub>2</sub>) composite membrane using a vacuum-assisted filtration method. The structural analysis confirmed that TiO<sub>2</sub> nanoparticles were uniformly distributed within the GO matrix, effectively expanding the interlayer spacing and enhancing hydrophilicity. These modifications led to a substantial improvement in water permeability and salt rejection, achieving over 99% NaCl rejection with a 125% increase in water flux compared to pristine GO membranes.

The improved performance can be attributed to the synergistic effects of TiO<sub>2</sub> nanoparticles acting as nano-spacers and hydrophilic agents, which minimized GO sheet restacking, increased water transport channels, and improved anti-fouling resistance. The composite membrane also exhibited enhanced thermal and mechanical stability, ensuring operational durability during desalination.

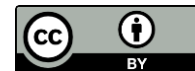
Overall, the GO–TiO<sub>2</sub> composite membrane demonstrates a strong potential for practical seawater desalination applications. Future work should focus on scaling up membrane fabrication and optimizing nanoparticle loading to further enhance flux-selectivity balance and long-term performance under real seawater conditions.

## REFERENCES

- Ali, M. E., Johnson, D. J., Arthanareeswaran, G., Ooi, B. S., & Shafi, H. Z. M. (2016). Structure–performance correlation of GO-based thin film nanocomposite membranes for desalination. *Desalination*, 386, 1–10. <https://doi.org/10.1016/j.desal.2016.02.015>
- Bhoje, R. S., Ghosh, A. K., & Nemade, P. R. (2022). Development of performance-enhanced graphene oxide-based nanostructured thin-film composite seawater reverse osmosis membranes. *ACS Applied Polymer Materials*, 4(2), 782–792. <https://doi.org/10.1021/acsapm.2c00094>
- Elzubair, A., Uchôa, L. R., & Prado da Silva, M. H. (2024). Production and characterization of graphene oxide/polymer support composite membranes for water desalination and purification. *Desalination and Water Treatment*, 322, 100012. <https://doi.org/10.1016/j.dwt.2024.100012>



- García-Picazo, F. J., Pérez-Sicairos, S., & Fimbres-Weihs, G. A. (2021). Preparation of thin-film composite nanofiltration membranes doped with N- and Cl-functionalized graphene oxide for water desalination. *Polymers*, 13(10), 1637. <https://doi.org/10.3390/polym13101637>
- Hassan, M. A., Hamdy, G., & Taher, F. A. (2024). Graphene oxide-enhanced polyethersulfone/polysulfone forward osmosis membranes for Suez Canal water desalination. *Polymer Engineering and Science*, 64(6), 26819. <https://doi.org/10.1002/pen.26819>
- Janwery, D., Memon, F. H., & Memon, A. A. (2023). Lamellar graphene oxide-based composite membranes for efficient separation of heavy metal ions and desalination of water. *ACS Omega*, 8(13), 18945–18956. <https://doi.org/10.1021/acsomega.2c07243>
- Kim, S., Lin, X., & Ou, R. (2017). Highly crosslinked, chlorine tolerant polymer network entwined graphene oxide membrane for water desalination. *Journal of Materials Chemistry A*, 5(7), 3432–3443. <https://doi.org/10.1039/C6TA07350F>
- Li, X., Zhu, J., Liu, Y., Wang, Y., & Cao, J. (2020). Enhancing desalination performance of graphene oxide membranes by controlled interlayer spacing and surface modification. *ACS Applied Materials & Interfaces*, 12(14), 16674–16684. <https://doi.org/10.1021/acscami.9b24134>
- Li, Z., Wang, Y., & Han, M. (2020). Graphene oxide incorporated forward osmosis membranes with enhanced desalination performance and chlorine resistance. *Frontiers in Chemistry*, 8, 877. <https://doi.org/10.3389/fchem.2019.00877>
- Liang, B., Zhan, W., & Qi, G. (2015). High performance graphene oxide/polyacrylonitrile composite pervaporation membranes for desalination applications. *Journal of Materials Chemistry A*, 3(7), 245–255. <https://doi.org/10.1039/C4TA06573E>
- Romaniak, G., Dybowski, K., & Jeziorna, A. (2020). Synthesis and characterization of semi-permeable graphene/graphene oxide membranes for water desalination. *Journal of Materials Science*, 55, 11683–11694. <https://doi.org/10.1007/s10853-020-04648-w>
- Shah, I. A., Bilal, M., & Ihsanullah, I. (2023). Revolutionizing water purification: Unleashing graphene oxide membranes. *Journal of Environmental Chemical Engineering*, 11(8), 111450. <https://doi.org/10.1016/j.jece.2023.111450>
- Solangi, N. H., Mubarak, N. M., & Karri, R. R. (2023). Holistic mechanism of graphene oxide and MXene-based membrane for desalination processes. *Desalination*, 558, 117035. <https://doi.org/10.1016/j.desal.2023.117035>
- Soomro, F., Ali, A., & Ullah, S. (2023). Highly efficient arginine intercalated graphene oxide composite membranes for water desalination. *Langmuir*, 39(49), 15122–15135. <https://doi.org/10.1021/acs.langmuir.3c02699>
- Tiwary, S. K., Singh, M., & Chavan, S. V. (2024). Graphene oxide-based membranes for water desalination and purification. *npj 2D Materials and Applications*, 8, 123. <https://doi.org/10.1038/s41699-024-00462-z>
- Wei, Y., Gao, X., & Xu, G. (2024). Laminated graphene oxide and hydrotalcite membranes via alternating spray-deposition with stable desalting performance. *Desalination*, 571, 117809. <https://doi.org/10.1016/j.desal.2024.117809>



Wu, X., Fang, F., & Zhang, K. (2017). Graphene oxide modified forward osmosis membranes with improved hydrophilicity and desalination performance. *Desalination and Water Treatment*, 64, 115–125. <https://doi.org/10.5004/dwt.2017.21227>